# Initial conceptual design and wing aerodynamic analysis of a solar power-based UAV

**W. Harasani**
**M. Khalid**
**mkholid@kau.edu.sa**
King Abdul Aziz University
Jeddah
Saudi Arabia

**N. Arai**
**K. Fukuda**
**K. Hiraoka**
Tokai University
Hiratsuka-city
Japan

## ABSTRACT

King Abdul Aziz University of Saudi Arabia (KAU) and Tokai University in Japan have collaborated to design and manufacture a solar powered unmanned air vehicle (UAV), Sun Falcon, which has capability of continuous one day flight with intended design extension towards night flight. The project is a student-driven endeavour involving some 30 students. Both universities are equally involved in the actual design studies of the performance characteristics, aerodynamic design, propulsion and structural analysis. Tokai University is in charge of the actual on-site supervision and examination of on-going manufacturing processes and ultimate fabrication of the prototype model.

The conceptual design of the Sun Falcon was meticulously worked out in consideration of the operational mission, which included such flight characteristics as the cruising velocity, flight altitude, payload, flight time, rate of climb, power requirements and so on. The weather condition patterns in Saudi Arabia, which remained fairly supportive of the solar cell performance, were also deemed crucial in the design process. However, the design of a solar plane had other challenges in terms of power unit accommodation and payload consideration in comparison to other conventional UAVs. In this paper, an outline of the design features of the Sun Falcon is presented and other notable design features particular to solar UAVs are discussed. It was learnt in this exercise that the selection of the base aerofoil is perhaps one of the most important design items, as the Reynolds number for such UAVs understandably drops notably lower than conventional aeroplanes and such features as the camber curvature and wing area must cater for the installation of solar panels

**Paper No. 3927.** Manuscript received 12 November 2012, revised version received 24 July 2013, accepted 12 December 2013. .

https://doi.org/10.1017/S0001924000009350 Published online by Cambridge University Press

whose size, strength and quantity must respect local weather conditions. For the Sun Falcon, the actual design process examined two candidate aerofoils FX74-CL5-140 (FX74) and SD7037-092-88(SD7037) both of which were abundantly suitable for furnishing the required aerodynamic characteristics. SD7037 was ultimately chosen as it provided the best geometry and camber line in terms of accommodation and placement of the solar panels. Further scrutiny demonstrated that this latter aerofoil provided better take-off performance and superior *L/D* behaviour under cruise conditions. In order to check out the aerodynamic performance in general and overall stability and control characteristics, a preflight test under battery power (a 2,500 mAh li-po 4-cell 14·8v) was achieved on 4 June 2013. Other solar powered based tests are currently under way at present.

# NOMENCLATURE

| | |
|---|---|
| $A$ | angle-of-attack |
| $b$ | full span of the main wing |
| $c$ | aerofoil chord length |
| $C_l$ | sectional lift coefficient |
| $C_L$ | lift coefficient, |
| $C_p$ | pressure coefficient |
| $D$ | drag |
| Eff | efficiency |
| $E$ | energy |
| $g$ | gravitational constant |
| $L$ | lift force per unit length |
| M | Mach number |
| $P$ | pressure |
| $P_\infty$ | freestream static pressure |
| Re | Reynolds number |
| $R/C$ | rate of climb (dH/dt) |
| Rad | radiation |
| $S$ | wing area |
| $s$ | semi span |
| $V$ | velocity |
| $T$ | thrust |
| $V_\infty$ | free-stream velocity |
| $W$ | weight (kg) |
| $x, y$ | co-ordinate system axis |
| $\theta$ | instantaneous inclination of the vehicle |
| $\rho^\infty$ | free-stream density |
| $\gamma$ | heat capacity ratio |

## Subscripts

| | |
|---|---|
| ave | average |
| req | required |
| init | initial |
| solar | solar conditions |
| cruise | cruising conditions |

https://doi.org/10.1017/S0001924000009350 Published online by Cambridge University Press

# 1.0 INTRODUCTION

UAVs have been on the aviation scene for the past two decades and have already proven their capabilities in a variety of missions, both for civilian and military purposes. They come in all shapes and sizes. At very low Reynolds number regimes $Re \leq 10^5$ with a total mass of $\leq 1$kg, the UAVs are considered to be micro unmanned air vehicle (MUAVs); and above this Reynolds number and mass regime they become mini to small sized UAVs and at still higher Reynolds numbers ($Re \geq 10^7$, $Mass \geq 10^3$) they are referred to as full-sized UAVs .The aerodynamics of mini to small sized vehicles, even when modelled on 2D aerofoils as discussed by Yuan and Khalid[1-3], is quite complex because the Reynolds number becomes low and flow separation often occurs even in laminar flight regimes leading to laminar flow separation bubbles with added stability and control challenges.

For UAVs which operate at very low Reynolds numbers ($Re\ 10^2 \sim 10^5$) under demanding navigational imperatives, the propulsion requirements become increasingly difficult to satisfy. There is a tendency to move towards a flapping wing concept, where the thrust and lift forces would be generated by the flapping wings and other appropriate pitch adjustment of the wing would facilitate the stability and control of such a vehicle. On the other hand, at higher Reynolds numbers, where the size of the vehicle becomes of the order of a couple of metres, other conventional types of UAVs become operative. The size, total weight and propulsion features of such a vehicle are determined based on the mission and payload requirements. The propulsion requirements as discussed by Logan *et al*[4] are satisfied by well integrated on-board propeller units furnished with rechargeable batteries. Elsewhere, solar powered batteries have also appeared in some recent designs. Only a few among them[5-7] have managed longer duration flights. Starting with Boucher's Sunrise[5] which flew for 20 minutes at an altitude of about 100m to Bruss and Militki's[6] Solaris which only managed a 150 second flight at an altitude of 50m. Beck's Solar Solitude[7] at 4lb in weight with a span of 108in and 8in chord flew at 25mph, powered by a Speed 500 motor. It used over 130 solar panels and was fitted with a Futaba auto-pilot to keep level at altitude. The present Sun Falcon sits very much among these preceding solar powered small sized UAVs, where the emphasis has been placed on sustained flight lasting many hours powered by efficient solar panels planted aloft the surface of the wing and able to continuously feed the efficient lithium batteries which furnish the propeller during the day and preserve energy for continuous flight into the night.

A large number of commercial companies have sprung up all over the world to supply such small to mid-sized UAVs, whether powered by conventional propeller-based systems or solar panel plus battery combinations to operate in a variety of civilian and military roles. In their civil missions they may be deployed in such roles as search, atmospheric pollution monitoring, forest fire monitoring, urban mapping, weather, coastal monitoring border patrol, narcotics prevention, surveillance of protracted areas etc. In terms of military deployments they could be used for intelligence gathering, surveillance for adversary movements, early warning look outs, etc. Mission deployment will, of course, dictate payload requirements. In Saudi terrain such UAVs could be extremely useful in inspecting vast expanses of the desert for water footprints or locating people and animals in distress or even monitoring large populations of people during the busy Hajj season. At much higher Reynolds numbers, the recent role of UAVs in Afghanistan has proven that such unmanned vehicles can be used against selected individuals or adversary groups with reduced risk to the military. Other full-scale UAVs, like the Stealth Bomber and Global Hawk, hold sway in such flight regimes which can respectively be used for large scale bombing over global distances or as remote surveillance platforms for monitoring and control of the aerial activity of a distant adversary.

https://doi.org/10.1017/S0001924000009350 Published online by Cambridge University Press

The Sun Falcon project was negotiated as a collaborative academic student project between King Abdul Aziz University in Saudi Arabia and Tokai University in Japan to design and manufacture a flight vehicle to operate at intermediate Reynolds numbers of about $4 \times 10^5$ and at a cruising velocity of about $16{\cdot}7 ms^{-1}$ at an altitude of about 100m. The paper addresses only the most important design features of this UAV and does not give a detailed description of the entire design and fabrication exercise. It is basically a demonstrative project to show that such a vehicle can be designed within the resources and manpower facilities in universities to address an important civilian requirement. The design strategies were especially focused to inspire local manufacturers to compete in a burgeoning international market. The conceptual design was based on the strategy proposed by Noth *et al*[7] and the design procedures were carefully selected to meet the defined mission. Starting the initial conceptual design from classic and ready estimates of aerodynamic performance, more accurate CFD simulations were adopted as the design matured. Such a vehicle was designed to remain airborne for long hours except for night flight with solar panels installed on the wing surface to charge up the batteries to operate during the day and store sufficient energy for flight into the night hours. A second generation of such a vehicle is envisioned for both day and night operations. While more rigorous testing of the solar panels for longer duration performance of the Sun Falcon is currently under way, the preliminary flight testing to examine the general aerodynamic performance and other stability and control behaviour was carried out in June 2013.

## 2.0 CRITICAL DESIGN ISSUES

The starting point of course is to strike a correct balance between the aerodynamic loads and the overall weight of the UAV. Some iterative parameter trading may be conducted throughout the design refining process. The mass balancing may have to contend with the energy demands of the vehicle, which in turn are directly related to the choice of batteries and number of solar panels. The design of the Sun Falcon demanded that the batteries and solar panels combination must furnish enough energy to maintain level flight at an altitude of about 100m during the day with enough energy stored to last the night hours. The total number of solar panels required, subject to their individual size may of course be restricted by the available wing surface area.

In level flight then, the aerodynamic lift has to at least to match the overall weight and the total drag has to be at least equal to the available thrust. Once the thrust requirements are established a good estimate of the power ($1/2\ \rho\ S\ V^3 C_D$) for the propulsion system become known. Thus one has to find an appropriate battery + solar panel combination as a propulsion supply unit must at least meet the weight requirements as dictated by the aerodynamic lift in level flight. The final element of the aerodynamic design deals with the rate of climb. Once all of the design criteria are met, the aerodynamic parameters together with weight and such dynamic parameters as the forward velocity and acceleration are fed into the rate of climb equation and as shown in Fig. 1, the design cycle is complete when all the constraints are appropriately satisfied.

Take-off and landing procedures are particularly important in UAV applications, as such vehicles often have to rely on simple and quick methods for immediate take-off to investigate or survey certain situations and then land comfortably even on rough landscapes with all data and equipment intact. Sun Falcon is equipped with two main undercarriage wheels under the wings and a third wheel for additional stability under the tail. It is designed for quick take-off from a small deck (< 30m) and landing on an airstrip of similar dimensions.

https://doi.org/10.1017/S0001924000009350 Published online by Cambridge University Press

## 3.0 INITIAL CONCEPTUAL DESIGN CYCLE

The initial design characteristics of the Sun Falcon were estimated simply by using the linear theoretical equations based on relationships given by Anderson[9]. The design cycle used in this stage of the study is shown in Fig. 1. In order to work through the various boxes in the design cycle, such aerodynamic features as the lift, skin friction, induced drag and power requirements for a given cruise velocity and aspect ratio were estimated from such relations as follows:

$$C_L = 2\pi\alpha \quad \ldots (1)$$

$$C_{Di} = \frac{C_L^2}{e\pi AR} \quad \ldots (2)$$

$$C_f = \frac{1{\cdot}328}{\sqrt{\mathrm{Re}}} \quad \ldots (3)$$

$$C_{D_{total}} = \frac{D}{\frac{1}{2}\rho V^2 S} = \frac{C_{D_i} + C_f}{0{\cdot}85} \quad \ldots (4)$$

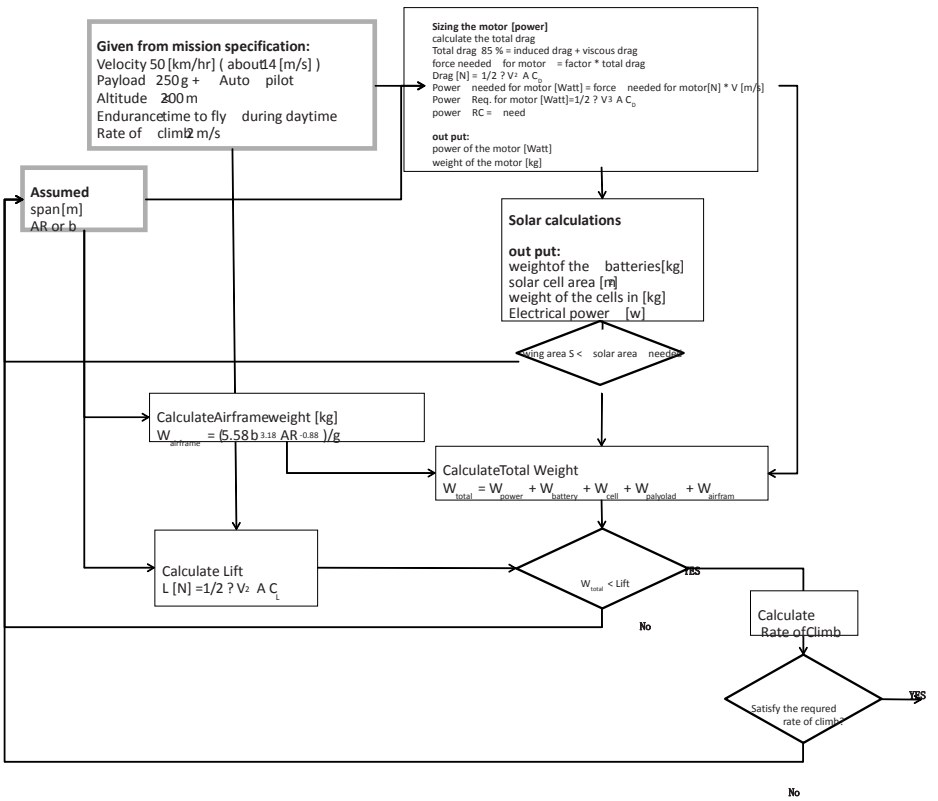



Figure 1. Preliminary design cycle for the Sun Falcon.

https://doi.org/10.1017/S0001924000009350 Published online by Cambridge University Press

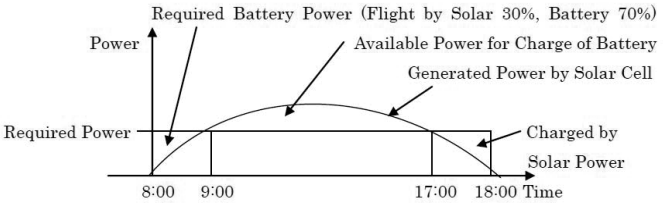



Figure 2. Distribution of energy balance.

Other weights for the airframe, battery and cell were estimated as follows:

$$\text{Total weight of solar modules (kgf)} = w_{sm} * S_{sm} \quad \ldots (5)$$

where $w_{sm}$ and $S_{sm}$ are a weight of solar module per unit area and a total area of solar modules, respectively. We assumed that $w_{sm} = 2{\cdot}0(\text{kgf}/\text{m}^2)$ because of an empirical value.

$$\text{Weight of battery (kgf)} = 1 \quad \ldots (6)$$

$$\text{Weight of airframe (kgf)} = 5{\cdot}58b^2 \frac{AR^{-0{\cdot}88}}{g} \quad \ldots (7)$$

The linear equations were iterated for a number of aspect ratio ($AR$) values in between 8 to 12 and the cruise velocity condition. The rate-of-climb criteria in the preliminary design cycle closed the prototype design cycle.

The energy requirements for the prototype were to be based upon the available power generation attributes of the solar panels. The average daily horizontal radiation 6,200 [Whr/m$^2$] for day time, as measured from July to September was obtained from a radiation measurement chart[6]. The energy balance in terms of the portion generated by the solar panels and the amount used up under flight conditions and the remaining portions used for charging up the battering and storage is shown diagrammatically in Fig. 2.

The power requirements can then be stated as follows:

$$P_{req} = \frac{T_{req} \cdot V_{cruise}}{Eff_{motor,gear\ head,prop}} \quad \ldots (8)$$

$$E_{solarcell} = Eff_{solar} \cdot Rad_{av} \cdot A_{solar} \quad \ldots (9)$$

The calculations of the rate of climb bare close relation to the power and available thrust. Starting from the equation of motion:

$$\frac{W}{g}\frac{\mathrm{d}V}{\mathrm{d}t} = T - D - W\,\mathrm{Sin}\,\theta \quad \ldots (10)$$

$$\frac{W}{g}\frac{\mathrm{d}\theta}{\mathrm{d}t} = L - W - \mathrm{Cos}\,\theta \quad \ldots (11)$$

Where d$V$/d$t$ is the acceleration (alpha). Therefore the required thrust is obtained using the rate of climb equation for $R/C$:

$$R/C = \frac{\mathrm{d}H}{\mathrm{d}t} = V\left(\frac{T-D}{W} - \frac{1}{g}\frac{\mathrm{d}V}{\mathrm{d}t}\right) \quad \ldots (12)$$

https://doi.org/10.1017/S0001924000009350 Published online by Cambridge University Press

$$T = D + W\left(\frac{\frac{R}{C}}{V} + \frac{1}{g}\frac{\mathrm{d}V}{\mathrm{d}t}\right) \quad \ldots (13)$$

Required time to cruising altitude is therefore given by:

$$T_{cruise} = \frac{\frac{H}{R}}{C} \quad \ldots (14)$$

The average acceleration is given by:

$$\frac{\mathrm{d}V}{\mathrm{d}t_{ave}} = \frac{\left(V_{cruise} - V_{init}\right)}{T_{cruise}} \quad \ldots (15)$$

Energy required to climb is calculated from the equation:

$$E_{climb} = \frac{P_{ave} \cdot T_{cruise}}{Eff_{motor} Eff_{gear\ head} Eff_{prop}} \quad \ldots (16)$$

Above relationship were used in a preliminary exercise for an aerofoil based two dimensional based wing, whose $C_L$ and $C_D$ characteristics were estimated from above simple lifting linear relationships. The first set of configuration design along with geometry, weight and propulsion and performance attributes are shown in Fig. 3.

As shown is Fig. 3, the span length and *AR* is 3·5m and 7·8, respectively. And the main wing has zero sweep-back and no taper. These parameter and feature of the geometry were decided by the consideration of the limitation of the manufacturing conditions. The UAV was designed to take-off on three wheels; two of which are placed directly under the main fuselage and the third is placed under the tail. The on-board battery which is energised non-stop in Arabian Sun was used to run the motor for take-off which was achieved within 10m of the start in the actual flight test.

# 4.0 INITIAL WING AERODYNAMIC DESIGN CYCLE

A more rigorous design cycle was undertaken to fine tune the above calculations using more accurate CFD based studies on typical aerofoil shapes which could be used as the base geometry for the main wing of the Sun Falcon. Towards this end a number of aerofoils were considered and finally the selection narrowed down to the FX74 and SD7037 aerofoils.

Tokai University and KAU conducted the 2D and 3D CFD calculations of the aerodynamic performance characteristics of both aerofoils. Under the 3D configuration the span length was kept 3·5m and the value of *AR* was fixed at 7·8.

## 4.1 Comparison of the performance between FX74 and SD7037

First, the characteristics of FX74 were confirmed as this aerofoil was known to have rather high coefficient of lift near stall. Although more comprehensive wind tunnel tests are currently underway at the Tokai, the performance needed to be confirmed at the precise operating condition with the ready numerical methods at hand. The 2D mesh of the FX74 aerofoil with 0·45 m chord length was created using PointWise mesh generator and calculations were performed by FLUENT under the conditions shown in Table 1.

https://doi.org/10.1017/S0001924000009350 Published online by Cambridge University Press

| Mission | |
|---|---|
| Cruising Velocity [km/hr] | 50.00 |
| Cruising Altitude H [m] | 100.00 |
| Payload [Kg] (Camera and Data Transmitter) | 0.60 |
| Flight Starting Time[h:m] | 9:00 |
| Flight Ending Time [h:m] | 17:00 |
| Endurance [h:m] | 8:00 |
| Rate of Climb R/C [m/s] | 2.00 |

| Configuration | |
|---|---|
| Wing Span [m] | 3.50 |
| Aspect Ratio [-] | 7.80 |

| Given Data | |
|---|---|
| Cruising $C_L$ | 0.50 |
| Oswald Efficiency Factor e (for High Mounted Wing) | 0.80 |
| Viscosity [Pa*s] | 0.0000182 |
| Sea Level Temperature To [K] | 288.00 |
| Gas Constant R[J/(K*kg)] | 287.00 |
| Decrease Rate of Temperature a [K/m] | 0.0065 |
| Sea Level Pressure $P_0$ [Pa] | 101325.00 |
| Sea Level Density $\rho_0$ [kg/m$^3$] | 1.226 |
| Efficiency of Motor(0.87) * Propeller(0.8) | 0.700 |
| Solar Cell Efficiency | 0.17 |
| Minimum Average Daily Horizontal Radiation [W*hr/m$^2$] | 4300.00 |
| Battery Weight [kg/(W*hr)] | 0.005 |
| Margin Time of Battery Usage [h:m] | 0:20 |

| Calculated Parameter | |
|---|---|
| Temperature T [K] | 287.35 |
| Pressure P [Pa] | 100128.19 |
| Density $\rho$ [kg/m$^3$] | 1.21 |
| Cruising Velocity [m/s] | 13.89 |
| Wing Area S [m$^2$] | 1.57 |
| Chord Length c [m] | 0.45 |
| Reynolds Number Re [-] | 4.158E+05 |
| Total Flat Plate Area [m$^2$] {Wing, Fuselage, Tail, and others (=2.6*Wing Area)} | 4.08 |
| Induced Drag Coefficient $C_{di}$ | 0.013 |
| Flat Plate Turbulent Viscous Drag Coefficient $C_{d0}$ | 0.00530 |
| Drag of Rest (interference etc.)[N] | 0.86 |
| Total Drag [N] | 5.74 |
| Number of Cell n | 26.00 |
| Number of cell m | 3.00 |
| Solar Panel Span Width [m] | 3.31 |
| Solar Panel Chord Length [m] | 0.39 |
| Solar Module Area [m$^2$] | 1.28 |

| Airframe | |
|---|---|
| Weight of Airframe [kg] (Incliding Weight of Motor, Controller, Propeller, Electric Circuit, and Actuator) | 5.02 |

| Motor and Propeller | |
|---|---|
| Required Thrust T [N] | 5.74 |
| Required Power [W] | 113.86 |
| Required Total Energy [W*hr] | 910.86 |

| Stalling Speed | |
|---|---|
| Airfoil | SD7037 |
| Maximum CL | 1.10 |
| Stalling Speed at Maximum CL and Sea Level [m/s] | 9.00 |

| Solar Cell | |
|---|---|
| Solar Cell Area [m$^2$] | 1.22 |
| Generated Energy in a Day [W*hr] | 890.91 |
| Weight of Solar Cell [kg] | 2.44 |
| Maximum Power from Solar Cell[W] | 174.93 |
| Critical Power for Battery Charge [W] | 126.82 |
| Time When Cell Power Exceeds Motor Power [h:m] | 10:48 |
| Time When Cell Power Falls Below Motor Power [h:m] | 15:11 |
| Aquired Battery Duration [h:m] | 1:48 |

| Battery | |
|---|---|
| Margin of Battery Energy [W*hr] | 37.95 |
| Required Total Battery Energy [W*hr] (Included Required Extra Energy) | 136.17 |
| Number of Li-ion Battery | 15 |
| Total Battery Weight [kg] | 0.68 |

| Energy Balance | |
|---|---|
| Available Total Energy [W*hr] | 1027.07 |
| Available Energy for Battery Charge [W*hr] | 116.22 |

| Weight Balance | |
|---|---|
| Margin of Weight [kg] | 0.00 |
| Total Weight W [kg] | 8.74 |
| Total Weight W [N] | 85.70 |
| Lift L [N] | 91.96 |
| Force Balance L-W [N] | 6.26 |

| Climb | | |
|---|---|---|
| Initial Velocity [m/s] | 7.50 | |
| Required Time to Cruising Altitude [s] | 50.00 | |
| Average Acceleration alpha[m/s$^2$] | 0.13 | |
| Required Thrust at V=7.5[m/s] [N] | 29.71 | [W] Required Power |
| at V=8.5[m/s] [N] | 27.02 | [W] |
| at V=9.5[m/s] [N] | 24.90 | [W] |
| at V=10.5[m/s] [N] | 23.18 | [W] |
| at V=11.5[m/s] [N] | 21.76 | [W] |
| at V=12.5[m/s] [N] | 20.57 | [W] |
| at V=13.5[m/s] [N] | 19.55 | [W] |
| at V=14.5[m/s] [N] | 18.68 | [W] |
| Required Energy [W*hr] | 4.90 | [W] Total |

Figure 3. Final design parameters of the Sun Falcon 1.

https://doi.org/10.1017/S0001924000009350 Published online by Cambridge University Press

**Table 1**
**The condition of 2D calculation for the aerofoils**

| | |
|---|---|
| Solver | SIMPLEC |
| Turbulent model | Spalart-Allmaras |
| Number of cells | 39,204 |
| Reynolds number | $4{\cdot}3 \times 10^5$ |
| Cruise velocity | $17 ms^{-1}$ |

As shown in Fig. 4, the maximum lift $C_{Lmax} = 1{\cdot}8$ could be obtained at about 10º of the angle-of-attack. But the lift curve slope is highly nonlinear while the lift remains positive at negative angles-of-attack. These tendencies must be attributed to the feature of notably large camber of the aerofoil. The increased camber must be inducing noticeable favourable circulation resulting in positive lift even at negative modest angles-of-attack. It is clear that there is a hint of a stall feature at negative angle-of-attack. Since there is small experimental data for this aerofoil, the analysis by the lifting line theory was carried out to further assess the lift ($C_L$) behaviour. The camber line for the FX74 aerofoil is approximated as:

$$Z = -1{\cdot}0947x^6 + 2{\cdot}8779x^5 - 3{\cdot}3922x^4 + 2{\cdot}717x^3 - 1{\cdot}7814x^2 + 0{\cdot}6702x - 0{\cdot}0028 \quad \ldots (17)$$

Glauert solution[11] derived from the lifting line theory provides an expression for the lift as:

$$C_L = \pi(2A_0 + A_1) \quad \ldots (18)$$

$$A_0 = \alpha - \frac{1}{\pi}\int_0^{\pi}\left(\frac{dz}{dx}\right)d\theta \quad \ldots (19)$$

$$A_1 = \frac{2}{\pi}\int_0^{\pi}\left(\frac{dz}{dx}\right)d\theta \quad \ldots (20)$$

$$\alpha_{C_{L=0}} = \frac{1}{\pi}\int_0^{\pi}\left(\frac{dz}{dx}\right)(1-\cos\theta)\,d\theta \quad \ldots (21)$$

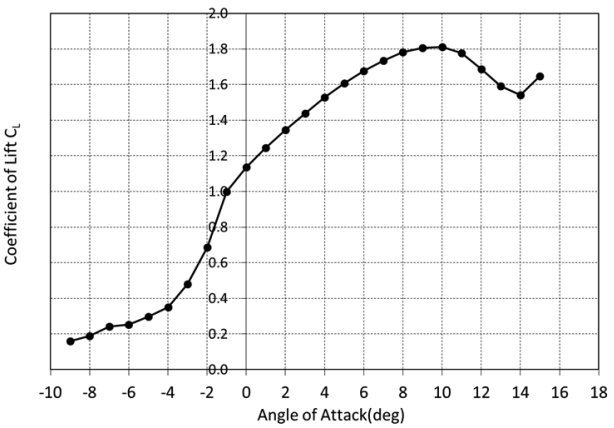



Figure 4. Coefficient of lift, $C_L$ *vs* angle-of-attack, α for FX74.

https://doi.org/10.1017/S0001924000009350 Published online by Cambridge University Press

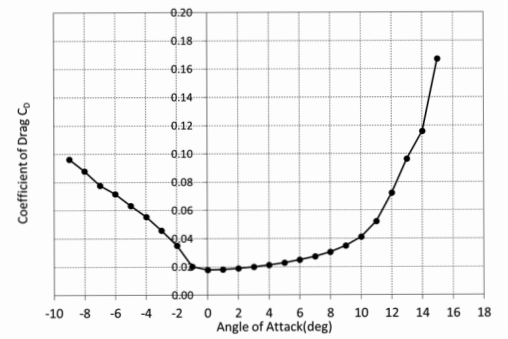



Figure 5. Coefficient of drag, $C_D$ *vs* angle-of-attack.

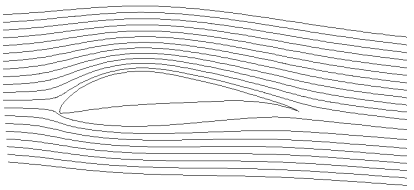


Figure 6(a). Stream line around FX 74 at α = 0º.

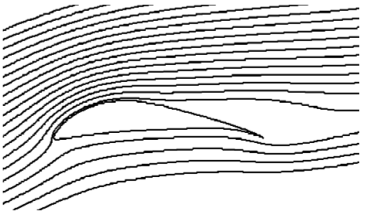


Figure 6(b). Stream lines around FX74 at α = 13º.

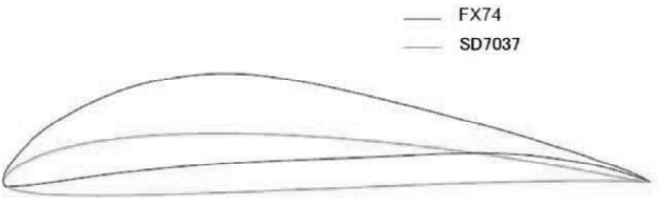



Figure 7. Comparison of the profiles between FX74 and SD7037.

Where $\alpha C_L = 0$ is the zero lift angle and it was evaluated to be $\alpha_{CL=0} = -11{\cdot}9°$.This result shows that the analytic value of $C_L$ agreed reasonably well with the result by CFD calculation.

The drag polar is shown in Fig. 5. The minimum drag coefficient is about 0·018. However, since $C_D$ polar increases rapidly as the angle-of-attack decreases towards negative, the range of the low drag ($6 \geq \alpha\,^{\circ} \geq 0$) is short. This means that the UAV would be restricted to remain within this limited range of angle-of-attack, if it seeks to fly most efficiently. FX74 aerofoil has other undesirable characteristics of $C_L$ and $C_D$ at the negative angle of attack at the Reynolds number around $4{\cdot}3 \times 10^5$. These tendencies were promoted by the flow separation at the leading edge of aerofoil on the upper surface. The flow fields as depicted by streamlines past the FX74 aerofoil as computed using Fluent computer code for angles-of-attack α = 0 and 13° condition are shown in Figs 6(a) and (b).

The flow separations occurred on the pressure surface fairly earlier own at about α = 0º and on the suction surface at α = 13º, respectively. It must also be noted that the tendency of rapid flow separation at increasing negative angles-of-attack produces the aforesaid nonlinearity of $C_L$ in lift curve slope and rapid growth of $C_D$.

https://doi.org/10.1017/S0001924000009350 Published online by Cambridge University Press

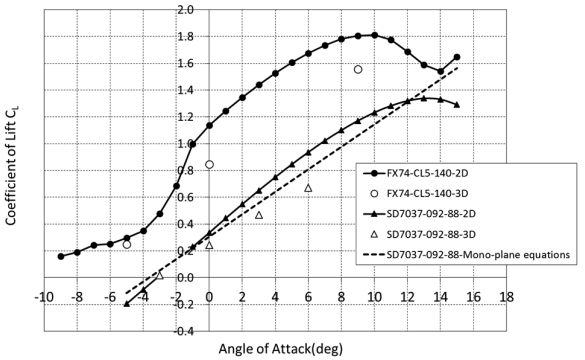



Figure 8. Coefficient of lift $C_L$ *vs* angle-of-attack α.

In an effort to arrive at the best possible aerodynamic lifting performance for the Sun Falcon, CFD calculations were now continued for the SD7037 aerofoil. Figure 7(b) compares the geometric profiles of both aerofoils.

It is clear that the curvature of camber of SD7037 is more modest than the one for the FX74 aerofoil which would lend itself to be more accommodating for the solar panels and sit more smoothly with the auxiliary equipment. Aerodynamic CFD simulations consistent with the above 2D computation on the FX87 aerofoil were also performed for the SD7037 aerofoil. See Fig. 8 for some of the Fluent-based results on the SD7037 aerofoil

With regards to the 3D CFD calculation, the 3D meshes would be configured very similarly with similar cross section for both FX74 or SD7037 aerofoils in the span wise direction. The thicknesses would respect the underlying aerofoil geometry and the wings were given zero taper and zero sweep-back. The span length was set at 3·5m with an aspect ratio of the straight wing of $AR = 7{\cdot}8$. The 3D grid for both models was generated almost identically with the total number of cells set at 2,365,400.The 3D calculations were carried out at only at specific significant angles of attack to obtain the various lift curve profiles. Results from the 3D calculation have been plotted in Fig. 8 which also show the comparison of performance of the two aerofoils.

Figure 8 shows the results of lift curve by 2D and 3D CFD calculation for the two aerofoils, FX74 and SD7037.Theoretical results based on the monoplane equation stated below is shown by broken line for only SD7037 aerofoil. The lift coefficient values for the FX74_CL5_140 aerofoil are much higher than the corresponding SD7037 aerofoil results but the former is noticeably non-linear which may not be an attractive feature from the stability and control point of view, where a linear behaviour of $C_L$ is desirable especially in the region of small negative angle of attack where the UAV may be expected to operate under cruise conditions. The SD7037 aerofoil displays attractive linear lift curve slope tendency. The monoplane based theoretical result remains very close to the CFD predictions for the SD7037 aerofoil. The monoplane equation based on the lifting line theory is used as follows[7]:

$$\sum_{\nu=1,3\ldots}^{N}\left(\frac{a_e C}{8S}n+\operatorname{Sin}\phi\right)a_n \operatorname{Sin} n\phi=\frac{a_e C}{8S}(\alpha-\alpha_{l0})\operatorname{Sin}\phi \qquad \ldots (22)$$

$$\frac{C_l}{C_L}=\frac{2A}{\pi SCA_1}\sum_{n-1,3\ldots}^{N}A_n \operatorname{Sin} n\phi \qquad \ldots (23)$$

Thus the sectional lift in terms of the overall lift on the wing at a given $C_L$ of 0·5 gives an elliptic loading as shown in Fig. 9.

https://doi.org/10.1017/S0001924000009350 Published online by Cambridge University Press

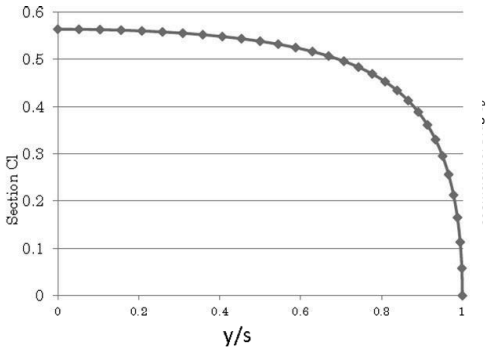



Figure 9. Sectional lift coefficient, $C_l$ *vs* span wise location *y*/s at $C_L$ = 0·5.

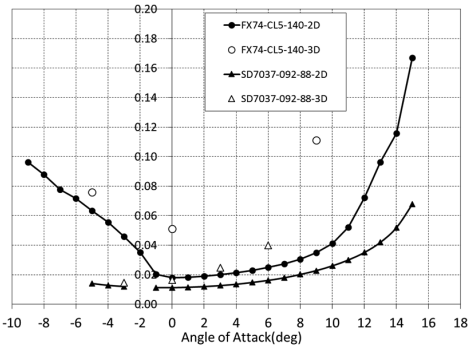



Figure 10. Coefficient of drag ($C_D$) *vs* angle-of-attack (α).

The drag polar corresponding to the above $C_L$ *vs* α curve shown in Fig. 8 is displayed in Fig. 10. The drag behaviour of the SD7037 aerofoil is far superior to the FX74 aerofoil. It is noted with satisfaction that SD7037 aerofoil maintains low drag behavior at virtually all angles of attack investigated. It is not surprising to note that drag coefficients obtained for 3D wings are consistently somewhat larger than their 2D counterparts. The tip vortices under a 3D configuration from straight sizeable wing tips give rise to a noticeable increase in induced drag.

Table 2 contains a more direct comparison between the FX74 and SD7037 aerofoils.

It is clear that the span length and AR parameters were driven by solar module size weight and geometry. This, invariably impacted upon the cruising speed and the $C_L$ requirements. As shown in Table 1, that at $C_L$ = 0·5, lift drag ratios of FX74 and SD7037are 11·4 at α = –3º and 42·4 at α = 3º, respectively. SD7037 thus has better gliding performance than the FX74 aerofoil. Furthermore, it is duly noted that, in the region of negative angle-of-attack, $C_L$ and $C_D$ of SD7037 aerofoil maintain their linearity, whereas $C_L$ and $C_D$ for FX74 become decidedly non-linear owing to the separation which occurs at the leading edge on the pressure side of FX74. From the viewpoint of the geometry, SD7037 has a very modest camber, which is highly desirable for the installing of solar panel. However, since the overall thickness over the chord of SD7037 aerofoil is less than the one of FX74 aerofoil, the main wing manufactured from SD7037 aerofoil, would have to be manufactured by a stiff material and structure so that the form sustains its shape.

## 5.0 FUSELAGE AND TAIL GEOMETRY

When considering the overall geometry for the Sun Falcon, the team looked at the dimensions of some of the contemporary UAVs operating at similar cruise velocities, altitudes and endurances. Table 3 itemises the geometries of some such UAVs.

**Table 2**
**Features of the FX74 and SD7037 aerofoils**

| | **FX74** | **SD7037-092-88** |
|---|---|---|
| $C_L/C_D$ ($C_L$ = 0·5) | 11·4 | 42·4 |
| $C_D$ | Higher | Lower |
| Curvature of camber | Larger | Smaller |
| | (Difficult to stick solar panels) | (Easy to stick solar panels) |

https://doi.org/10.1017/S0001924000009350 Published online by Cambridge University Press

Based on a study of aforementioned UAVs, the span/length ratio for the Sun Falcon was set to remain in between 1·7 to 2·6m, providing a fuselage length domain in between 1·35 to 2·05m.

Using the sizing data for light 2-4 seats engine aeroplanes as an example, the volume ratios of horizontal and vertical tails were designed for a good static stability as follows. For the horizontal tail then we have the relationship:

$$\frac{S_H}{S_W} * \frac{l_H}{C} > 0 \cdot 6 \quad \ldots (24)$$

Where,

$S_H$ area of horizontal tail
$S_w$ area of wing
$l_H$ distance from the center of gravity (tail arm)
$c$ chord length

For the vertical tail we have the equivalent relationship:

$$\frac{S_V}{S_W} * \frac{l_v}{b} > 0 \cdot 055 \quad \ldots (25)$$

Where,

$S_v$ area of vertical tail
$l_v$ distance from the centre of gravity (tail arm)
$b$ span of the wing

Assuming the distance from the centre of gravity to tail to be 1·0 to 1·5 [m], tail area was estimated as shown in Table 4, where *Sw* is 1·57 [m$^2$], *c* is 0·45 [m] and *b* is 3·5 [m] in the above equations for horizontal and tail geometries. Table 4 provides a comprehensive guideline towards arriving at the most efficient empennage configuration.

## 6.0 INITIAL FLIGHT TESTS

The Sun Falcon 1 project was completed in June 2013, with the first successful test flights conducted during 6-9 June 2013. The UAV in flight is shown in Fig. 11. Some of the lessons learnt from the flight tests included the following:

**Table 3**
**Physical dimensions of contemporary UAV**

| Aeroplane | Span b[m] | Chord c[m] | Length [m] | Wing area [m$^2$] | AR [-] | Weight [kg] | Span/length [m] |
|---|---|---|---|---|---|---|---|
| Solus Solar | 3·2 | 0·29 | 0·88 | 0·93 | 11 | 2·2 | 3·64 |
| Poly | 3·24 | 0·29 | 0·88 | 0·97 | 11 | 2·5 | 3·68 |
| Solar Silberfucls | 4·0 | 0·25 | 1·52 | 1·0 | 16 | 2·1 | 2·63 |
| Slamax | 3·48 | 0·3 | 1·59 | 1·04 | 11·6 | 2·54 | 2·19 |
| Solariane | 3·08 | 0·28 | 1·72 | 0·85 | 11·2 | 1·8 | 1·79 |
| Sky Sailor | 3·2 | 0·24 | 1·82 | 0·78 | 13·2 | 2·5 | 1·76 |

https://doi.org/10.1017/S0001924000009350 Published online by Cambridge University Press

**Table 4**
**Area of tail**

| | Horizontal tail Volume ratio | | | Vertical tail Volume ratio | | |
|---|---|---|---|---|---|---|
| | **0·6** | **0·65** | **0·07** | **0·055** | **0·06** | **0·065** |
| **Tail arm (m)** | **Area of tail ($m^2$)** | | | **Area of tail ($m^2$)** | | |
| 1 | 0·404 | 0·438 | 0·471 | 0·295 | 0·321 | 0·348 |
| 1·1 | 0·367 | 0·398 | 0·428 | 0·268 | 0·292 | 0·316 |
| 1·2 | 0·337 | 0·365 | 0·393 | 0·245 | 0·268 | 0·29 |
| 1·3 | 0·311 | 0·337 | 0·362 | 0·227 | 0·247 | 0·268 |
| 1·4 | 0·289 | 0·313 | 0·337 | 0·21 | 0·23 | 0·249 |
| 1·5 | 0·269 | 0·292 | 0·314 | 0·196 | 0·214 | 0·232 |

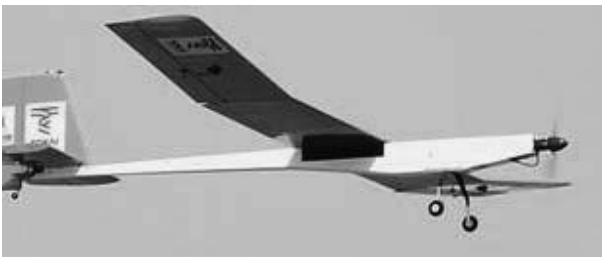


Figure 11. Sun Falcon 1 in full flight during the first test runs.

The overall weight of the UAV was monitored with meticulous care throughout the fabrication stages. The energy balance too was established accurately during the design phases.

It is proposed that the S9352 HV high torque Futaba servos should be used in order to avoid a situation where the RC glider would not respond when controlled in flight. The use of a closed-loop system on the rudder and elevator controls was strongly recommended as the servos were more than 1,300mm away from the controls' hinge point.

It was recommended to replace li-po batteries in place of li-ion version as they would be more suitable for the longer duration flight.

It was learnt that the brushless motor's capacity of 810kV was too high a kV for the 17 × 12 propeller, and this created the heat due to the overload from the propeller. After conducting numerous on-ground tests with the same 810kV motor and a smaller propeller and also with a 350kV motor it was decided to fly Sun Falcon 1 with a 350kV motor, and a 17 × 12 propeller with a li-po or li-ion battery.

For the overall design concept, the first flight tests confirmed that the prototype performed according to intended design. Further collection of data on such parameters as speed, altitude, power required by motor, propeller revs/sec, energy generated by solar modules and so on, during cruising flight and their respective comparison against design values will determine the need to further fine tune our design formulae. Weight estimate techniques certainly warrant modification as the weight of the airframe as the actual weight was somewhat heavier than design one.

## 7.0 CONCLUSION

The Sun Falcon wing has been designed starting from the rudimentary analysis of a conceptual configuration based on classic methods. More accurate design procedures, based on accurate

https://doi.org/10.1017/S0001924000009350 Published online by Cambridge University Press

CFD analysis were adopted towards the final design iterations. The design at hand provides for a cruise velocity of about 17ms$^{-1}$ at an altitude of 100m with a minimum endurance of about 10 hours, although continuous recharging of batteries in the Saudi climate would provide for virtually non-stop day/night operations. The longer duration flight has been designed to be made possible by efficient operation of the solar panels reputed to be capable of consistent charging of the batteries from prolonged daylight sun exposure. While the staff and students from both institutions participated in the overall design over long distance teleconference meetings, the majority of the manufacturing was carried out at the Tokai University in Japan.

Collaboration continues between the King Abdul Aziz University of Saudi Arabia and the Tokai University of Japan calls for a second generation design and manufacture of Sun Falcon 2 capable of continuous flight operations lasting many days and nights. The above lessons learnt, particularly in the area of weight management, would be extremely important in order to keep the weight within design limits. Sun Falcon 2 would have to support larger wings in order to accommodate a bigger solar panel area. The flight tests from Sun Falcon 1 would be used to calibrate precisely the number of solar panels required. Equally, the motor capacity would be worked out accurately based on the data from Sun Falcon 1 to avoid heating issues. For better control during flight, due attention would be focused on the closed loop system on the rudder for a better response. Further study of data from flight tests and continuing wind-tunnel experiments suggest that the V-shaped tail design would offer better prospects. It has further been recommended that li-ion batteries would be better suited for the longer duration flight intended for Sun Falcon 2, than the first set of li-po batteries installed on Sun Falcon 1.

## ACKNOWLEDGEMENT

The project was funded by the Deanship of Scientific Research (DSR), King Abdul Aziz University, Jeddah, under the Grant No. (431/009). The authors therefore acknowledge with thanks DSR technical and financial support, and furthermore the authors would like to express their gratitude and appreciation to Tokai University for their technical help and support.

## REFERENCES

1. YUAN, W. and KHALID, M. Insect sized flapping wing UAVs, *Int J Micro Vehicles*, 17 March 2010.
2. YUAN, W. and KHALID, M. Preliminary CFD studies of flapping wing aerodynamics, *Canadian Aeronautics and Space J*, 6 March 2008, **54**, (3/4), pp 51-63.
3. YUAN, W. and KHALID. M. 5.4 Numerical methods for plunging and flapping wings, 5.4.3 IAR Approach, AVT-101 Final Report (Experimental and Computational Investigations in Low Reynolds Number Aerodynamics, with Applications to Micro Air Vehicles), 8 April 2006.
4. LOGAN, M.J., CHUZ, J., MOTTERS, M.A, CARTER, D.L., OL, M. and ZEUNE, C. Small UAV research and evolution in long endurance electric powered vehicles, AIAA Conference 2007.
5. BOUCHER, R.J. History of solar flight, 1984, AIAA Paper 84-1429.
6. BRUSS, H. Solar ModellflugGrundlagen, 1991, Enwicklung, Praxis, VerlagfürTechnik und handwerk, Baden-Baden, Germany.
7. BECK, D. Solar Solitude, 1996, http://personalpages.tds.net/~dbeck/
8. NOTH, A., SIEGWART, R. and ENGEL, W. Design of solar-powered airplanes for continuous flight, December 2007, given in the framework of the ETHZ lecture Aircraft and Spacecraft Systems: Design, Modeling and Control, partially included in a forthcoming Springer book on *Advances in Unmanned Aerial Vehicles, State of the Art and the Road to Autonomy*.
9. ANDERSON, J.D. *Introduction to Flight*, Second Edition, 1985, McGraw-Hill Book Co, New York, USA.
10. HARASANI, W. Private Communication, 2012, Radiation measurement charts in Saudi Arabia.
11. GLAUERT, H. *The Elements of Aerofoil and Air Screw Theory*, Second Edition, Cambridge University Press, UK.

https://doi.org/10.1017/S0001924000009350 Published online by Cambridge University Press